Free convection heat transfer and entropy generation analysis of water-Fe_3O_4/CNT hybrid nanofluid in a concentric annulus

Abstract

Purpose- This work aims to numerically investigate the heat transfer and entropy generation characteristics of water-based hybrid nanofluid in natural convection flow inside a concentric horizontal annulus.

Design/Methodology/approach- The hybrid nanofluid is prepared by suspending tetramethylammonium hydroxide (TMAH) coated Fe_3O_4 (magnetite) nanoparticles and gum arabic (GA) coated carbon nanotubes (CNTs) in water. The effects of nanoparticles volume concentration and Rayleigh number on the streamlines, isotherms, average Nusselt number as well as the thermal, frictional and total entropy generation rates are investigated comprehensively.

Findings- Results show the advantageous effect of hybrid nanofluid on the average Nusselt number. Furthermore, the study of entropy generation shows the increment of both frictional and thermal entropy generation rates by increasing Fe_3O_4 and CNTs concentrations at various Rayleigh numbers. Increasing Rayleigh number from 10^3 to 10^5, at Fe_3O_4 concentration of 0.9% and CNT concentration of 1.35%, increases the average Nusselt number, thermal entropy generation rate, and frictional entropy generation rate by 224.95%, 224.65%, and 155.25%, respectively. Moreover, increasing the Fe3O4 concentration from 0.5 to 0.9%, at Rayleigh number of 10^5 and CNT concentration of 1.35%, intensifies the average Nusselt number, thermal entropy generation rate, and frictional entropy generation rate by 18.36%, 22.78%, and 72.7%, respectively.

Originality/Value- To the best knowledge of the authors, there are not any archival publications considering the detailed behaviour of the natural convective heat transfer and entropy generation of hybrid nanofluid in a concentric annulus.

Keywords: Hybrid nanofluid, Natural convection, Entropy generation, Fe_3O_4, CNT, concentric annulus

1. Introduction

The problem of natural convection heat transfer in concentric and eccentric cylindrical annulus has been attracting lots of attention due to its wide applications including heat exchangers, thermal storage systems, solar collectors, water distillation and underground electric transmission cables (Garg and Szeri, 1992; Khanafer and Chamkha, 2003; Ghernoug et al., 2016; Mahmoud Aly and Asai, 2016; Afrand et al., 2017, Alipour et al, 2017). However, modifying the heat transfer characteristics in the natural convection flows in the annulus is always sought out due to a large number of applications (Afrand, 2017; Abhilash and Lab, 2018; Zhao et al., 2018, Mashayekhi et al., 2017). As one of the first studies, Crawford and Lemlich (Crawford and Lemlich, 1962) studied the laminar natural convection flow between concentric circular annulus for several diameter ratios and Grashof numbers at a constant Prandtl number. Kuehn and Goldstein (1976, 1978) performed an investigation on natural convection within a horizontal annulus. Different fluids of water and air were examined for various Rayleigh numbers considering constant thermophysical properties. They reported good agreement between the numerical and experimental results. Dutta et al. (2018) investigated the impacts of tilt angle and fluid yield stress on the natural convection from an isothermal square bar in a square annulus. They considered the effects of Rayleigh number, Prandtl number, Bingham number, aspect ratio, and angle of inclination. The results showed that the Nusselt

number increases with increasing the Rayleigh number and decreases with increasing Bingham number. Imtiaz and Mahfouz (2018) studied the natural convection flow in an eccentric annulus containing heat-generating fluid. They found that the average dimensionless temperature of the fluid intensifies with the increase in the heat generation parameter. Besides, it was reported that the rate of heat transfer reduces for a fixed Rayleigh number as the inner cylinder moves upward from negative eccentricity to positive eccentricity.

Heat transfer enhancement, especially in natural convection systems, is important for energy saving purposes in industries (Eckert et al., 1987, Pourfattah et al., 2017, Rezaei et al., 2017). The main limitation of conventional heat transfer fluids is their low thermal conductivity which has a high effect in natural convection systems (Parvin et al., 2012, Akbari et al., 2016, Sajadifar et al., 2017). Nanofluids have been used widely in the last two decades as one of the advantageous methods to increase the heat transfer in different energy systems (Putra et al., 2003, Akbari et al., 2015, Arabpour et al., 2018a, Shamsi et al., 2017). By using nanoparticles in a base fluid, the heat transfer characteristics of the employed fluid can be modified (Vadasz et al., 2005, Akbari et al., 2017, Arabpour et al., 2018b, Heydari et al,, 2017, Zadkhast et al., 2017). There have been lots of studies on the heat transfer enhancement in natural convection problems in the literature using nanofluids. Cadena-de la Peña et al. (2017) examined different mineral oil-based nanofluids as a cooling fluid in an annulus between two cylinders and showed heat transfer enhancement by the newly generated nanofluids. The inner cylinder acted as a heat source while the outer one remained at a constant temperature. AIN and TiO_2 nanoparticles were added to the oil-based fluid with various concentrations with and without oleic acid treatment. They presented correlations for the Nusselt number in terms of Rayleigh number. Selimefendigil and Oztop (2017) numerically assessed the natural convection heat transfer of water-CuO nanofluid in a horizontally partitioned annulus in the presence of an inclined magnetic field. They considered a conductive partition with different thickness and thermal

conductivity. The results demonstrated that the heat transfer enhances by increasing the thickness of the conductive partition, Rayleigh number and inclination angle while reduces by decreasing Hartmann number. Siavashi and Rostami (2017) numerically examined the natural convection heat transfer of non-Newtonian water-Al_2O_3 nanofluid within a cylindrical annulus with a concentric circular heat source covered with a conductive porous layer. The results revealed that the non-Newtonian nanofluid has a higher Nusselt number than the other studied cases. Li et al. (2018) investigated the influence of radiative heat transfer on magnetohydrodynamic free convection of a water-Fe3O4 nanofluid in a sinusoidal annulus. They showed a decrease in the average Nusselt number with the increase of buoyancy force, Hartmann number and numbers of undulations. Miroshnichenko et al. (2018) studies natural convection in an open inclined cavity for cooling heat generation elements using a water-Al_2O_3 nanofluid. They studied different effective parameters of the system in order to minimize the average temperature of the heater and showed the advantageous effect of alumina nanoparticles in the base fluid.

To the best knowledge of the authors, there are not any archival publications considering the detailed behaviour of the natural convective heat transfer and entropy generation of hybrid nanofluid in a concentric annulus. In this paper, the problem of two-dimensional natural convection of water-Fe_3O_4/CNT hybrid nanofluid between two horizontal concentric cylinders is investigated. The inner cylinder surface is kept at a constant temperature which is higher than the outer cylinder temperature. The effects of nanoparticles volume concentration and Rayleigh number on the streamlines, isotherms, average Nusselt number as well as the local and global thermal entropy generation rate, frictional entropy generation rate and total entropy generation rate are analysed.

2. Physical properties of nanofluid

The water-based hybrid nanofluid containing TMAH coated Fe_3O_4 nanoparticles and GA coated CNTs is synthesized by mixing the required amount of water-Fe_3O_4 nanofluid and water-CNT nanofluid, followed by sonication of the mixture for 5 min. The water-Fe_3O_4 nanofluid was prepared by utilizing the technique proposed by Berger et al. (1999) and the water-based CNT nanofluid was synthesized via the method described by Garg et al. (2009). The details of the preparation and characterization of the hybrid nanofluid can be found in the author's previous work (Shahsavar et al., 2016). The interaction between the TMAH and GA molecules results in the physical attachment of the Fe_3O_4 and CNT nanoparticles.

After careful preparation and characterization, a series of experiments were carried out to obtain the thermophysical properties of the hybrid nanofluids containing different concentrations of the Fe_3O_4 and CNT nanoparticles. The volume concentration of the Fe_3O_4 and CNT nanoparticles in the prepared nanofluid samples as well as the density (ρ_{nf}), specific heat ($c_{p,nf}$), viscosity (η_{nf}), thermal conductivity (k_{nf}) and thermal expansion coefficient (β_{nf}) of these hybrid nanofluids are presented in Table 1.

Table 1. Characteristics of the studied nanofluid samples.

sample name	Fe_3O_4 vol.%	CNT vol.%	ρ_{nf} (kg/m^3)	$c_{p,nf}$ (J/kgK)	η_{nf} (kg/ms)	k_{nf} (W/mK)	β_{nf} (1/K)
0.5%FF	0.5	0	1016.77	4093.83	0.001042	0.695	0.000256
0.7%FF	0.7	0	1024.67	4060.29	0.001300	0.728	0.000255
0.9%FF	0.9	0	1032.58	4027.27	0.001534	0.749	0.000254
0.9%FF+0.45%CNT	0.9	0.45	1037.54	3996.40	0.001755	0.839	0.000253
0.9%FF+0.9%CNT	0.9	0.9	1042.50	3965.83	0.001804	0.856	0.000252
0.9%FF+1.35%CNT	0.9	1.35	1047.47	3935.55	0.001855	0.887	0.000251

3. Model configuration

3.1. Geometry and boundary conditions

The nanofluid is considered incompressible and the flow is considered to be laminar and steady-state. The outer cylinder with the radius of r_o is cooled at the temperature of T_c and the inner cylinder with the radius of r_i is kept at the hot temperature of T_h. The schematic of the problem is demonstrated in Fig. 1.

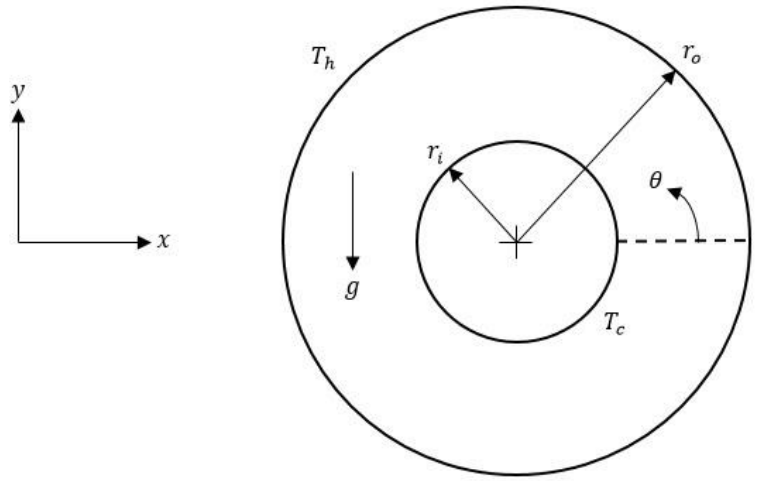

Fig. 1

3.2. Governing equations

In order to numerically investigate the natural convection heat transfer behaviour of the studied nanofluids in a concentric annulus, the conservation of mass, momentum and energy should be solved. The assumptions considered in the study are as follows:

(a) The thermophysical properties of the hybrid nanofluid are constant except for the density variation.

(b) The Boussinesq approximation is employed to consider the effect of natural convection.

(c) The hybrid nanofluid behaves like a homogeneous single phase fluid.

The governing equations for conservation of mass, momentum, and energy, based on the assumptions given above can be expressed as below:

(i) Conservation of mass,

$$\frac{\partial v_x}{\partial x} + \frac{\partial v_y}{\partial y} = 0 \tag{1}$$

(ii) Conservation of momentum in the x-direction,

$$\rho_{nf}\left(v_x\frac{\partial v_x}{\partial x} + v_y\frac{\partial v_x}{\partial y}\right) = -\frac{\partial p}{\partial x} + \eta_{nf}\left(\frac{\partial^2 v_x}{\partial x^2} + \frac{\partial^2 v_x}{\partial y^2}\right) \tag{2}$$

(iii) Conservation of momentum in the y-direction,

$$\begin{aligned}\rho_{nf}&\left(v_x\frac{\partial v_y}{\partial x} + v_y\frac{\partial v_y}{\partial y}\right)\\ &= -\frac{\partial p}{\partial y} + \eta_{nf}\left(\frac{\partial^2 v_y}{\partial x^2} + \frac{\partial^2 v_y}{\partial y^2}\right) - \rho_{nf}g\left[1 - \beta_{nf}(T - 298)\right]\end{aligned} \tag{3}$$

(iv) Conservation of energy,

$$\rho_{nf}c_{p,nf}\left(v_x\frac{\partial T}{\partial x} + v_y\frac{\partial T}{\partial y}\right) = k_{nf}\left(\frac{\partial^2 T}{\partial x^2} + \frac{\partial^2 T}{\partial y^2}\right) \tag{4}$$

where v_x is the x component velocity, v_y is the y component velocity, p is the pressure, g is the gravitational acceleration, and T is the temperature.

3.3. Data reduction

The Rayleigh number for pipe flow is defined by the following equation:

$$Ra = \frac{g\beta_{nf}(T_h - T_c)(r_o - r_i)^3\rho_{nf}^2 c_{p,nf}}{\eta_{nf}k_{nf}} \tag{5}$$

The average convective heat transfer coefficient at the inner annular wall is defined as:

$$h = \frac{\dot{Q}}{2\pi r_i(T_h - T_c)} \tag{6}$$

where $\dot{Q}$ is the heat transfer rate.

The convective heat transfer coefficient is also defined in the form of Nusselt number as:

$$Nu = \frac{h(r_o - r_i)}{k_w} \tag{7}$$

where k_w is the thermal conductivity of water at 25 ℃.

3.4. Entropy generation

The entropy generation in the flow field comprises of two main parts; (i) frictional factors, and (ii) thermal irreversibility. The local thermal and frictional entropy generation rates can be obtained as,

$$\dot{S}'''_{g,h} = \frac{k_{nf}}{T^2}\left[\left(\frac{\partial T}{\partial x}\right)^2 + \left(\frac{\partial T}{\partial y}\right)^2\right] \tag{8}$$

$$\dot{S}'''_{g,f} = \frac{\eta_{nf}}{T}\left\{2\left[\left(\frac{\partial v_x}{\partial x}\right)^2 + \left(\frac{\partial v_y}{\partial y}\right)^2\right] + \left(\frac{\partial v_x}{\partial y} + \frac{\partial v_y}{\partial x}\right)^2\right\} \tag{9}$$

Moreover, the total entropy generation rate ($\dot{S}'''_{g,t}$) is obtained by the following equation:

$$\dot{S}'''_{g,t} = \dot{S}'''_{g,h} + \dot{S}'''_{g,f} \tag{10}$$

The global entropy generation rates are calculated by the integration of the local entropy generation rates over the whole domain as follows:

$$\dot{S}_{g,f} = \int \dot{S}'''_{g,f}\, dV, \quad \dot{S}_{g,h} = \int \dot{S}'''_{g,h}\, dV, \quad \dot{S}_{g,t} = \int \dot{S}'''_{g,t}\, dV \tag{11}$$

3.5. Numerical method and validation

In this contribution, ANSYS-FLUENT computational fluid dynamics (CFD) software incorporated with a finite volume method is utilized to solve the governing equations along with the mentioned boundary conditions. The second order upwind method is used for solving the momentum and energy equations. Pressure and velocity are coupled using Semi-Implicit

method for Pressure-Linked Equations (SIMPLE) algorithm. For all parameters, the convergence criteria is set to 10^{-6}.

Five different grids were considered to check grid independency of the numerical results. Owing to severe velocity and temperature gradients adjacent to the walls, smaller elements were applied in the near wall region. Eventually, a grid with 400 nodes in the circumferential direction and 45 nodes in the radial direction was selected as the best one (see Fig. 2).

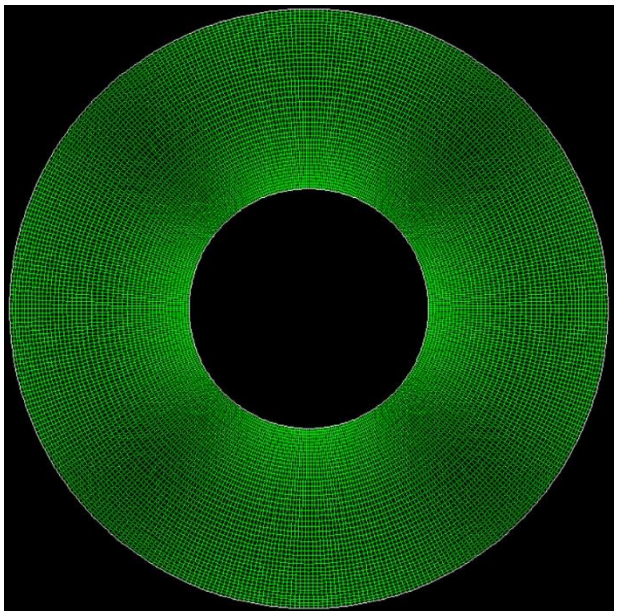

Fig. 2

Validation of the numerical analysis is accomplished by comparing the obtained numerical data for the temperature profile with the experimental results of Kuhen and Goldstein (1976) for the flow of water in an annulus using $Ra = 4.57 \times 10^4$ and $Pr = 0.7$. The comparison for three temperature profiles at three different angles is illustrated in Fig. 3. It can be seen that there is good agreement between the results.

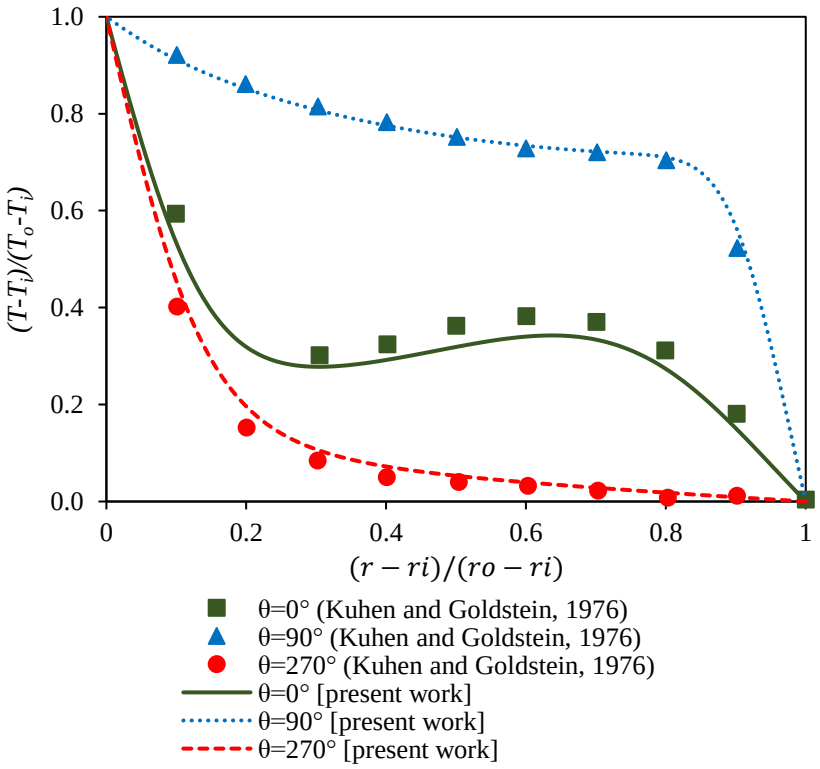

Fig. 3

4. Results and discussion

In the current investigation, the analysis is carried out to evaluate the influences of nanoparticle volume concentration and Rayleigh number on the heat transfer and entropy generation characteristics of the water-Fe_3O_4/CNT hybrid nanofluid flowing through a horizontal concentric annulus. The numerical simulations are performed at Fe_3O_4 concentrations of 0.1-0.9%, CNT concentrations of 0.45-1.35% and Rayleigh numbers of 10^3-10^5.

In order to obtain insight into the detailed flow structures, initially, streamlines (left) and isotherms (right) patterns for the natural convection flow of pure water, 0.9%FF and 0.9%FF+1.35%CNT at Rayleigh numbers of 10^3, 10^4 and 10^5 are presented in Figs. 4-6, respectively. The fluid near the inner hot surface moves upward while the fluid near the outer surface moves downward. This recirculation occurs as the two boundary layers of the inner and outer surfaces merge, creating the so-called kidney-shaped core or cellular configuration. With increasing the Rayleigh number, the density of streamlines increases on the upper surface of

the inner cylinder indicating a stronger natural convection flow. In addition, the comparison of streamlines related to different fluids at different Rayleigh numbers reveals that by increasing the volume fraction of nanoparticles, the maximum strength of streamlines increases due to the enhancement of the thermal conductivity of nanofluids. In the case of law Rayleigh number (10^3), the isotherms are nearly concentric indicating the small effect of the convective flow on heat transfer rate. With increasing the Rayleigh number, the circles gradually move away from the centre and lose their circular shape and the plume region is created and extended. Increasing the concentration of nanoparticles leads to an increase in the viscosity and, as a result, a decrease in the movement of the fluid which results in a reduction in the heat transfer and a decrease in the area of plume region. On the other hand, increasing the concentration of nanoparticles leads to an increase in the thermal conductivity, which causes a higher heat transfer and a wider plume region. In low Rayleigh numbers, due to the weakness of convection and the great role of conduction heat transfer, the effect of thermal conductivity enhancement overcomes the viscosity enhancement, and the area of plume region decreases for the higher concentration of nanoparticles, while the opposite is true for the large Rayleigh numbers.

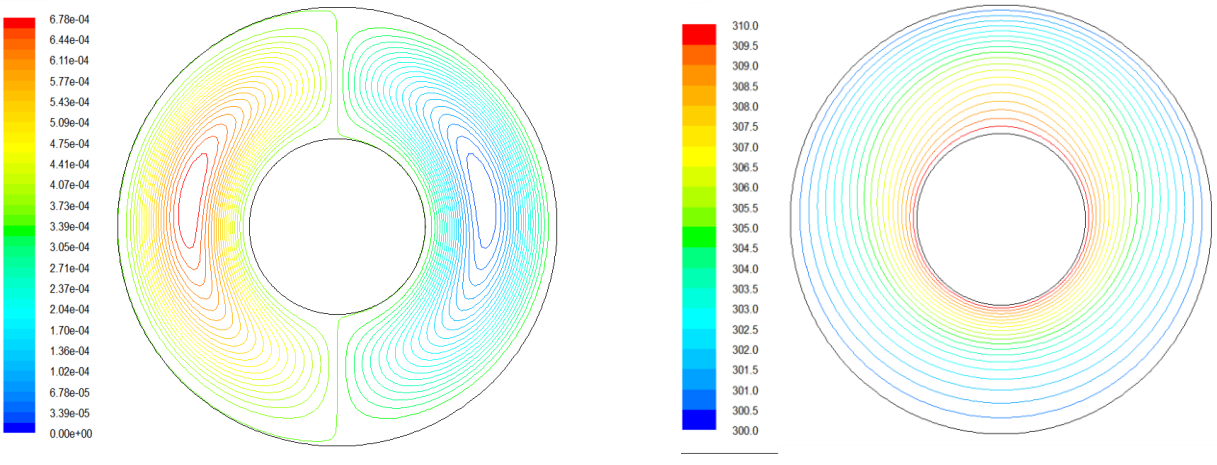

(a)

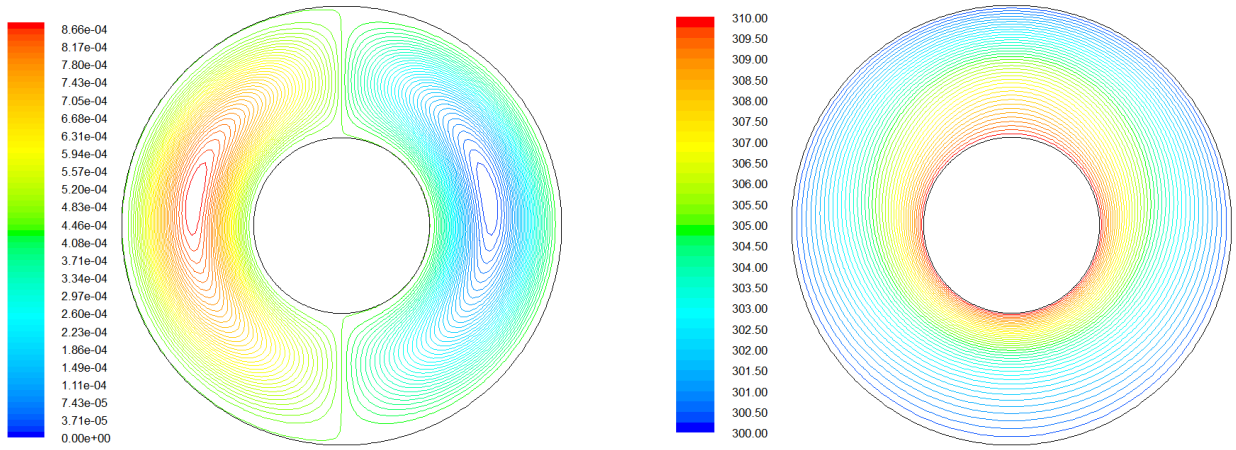

(b)

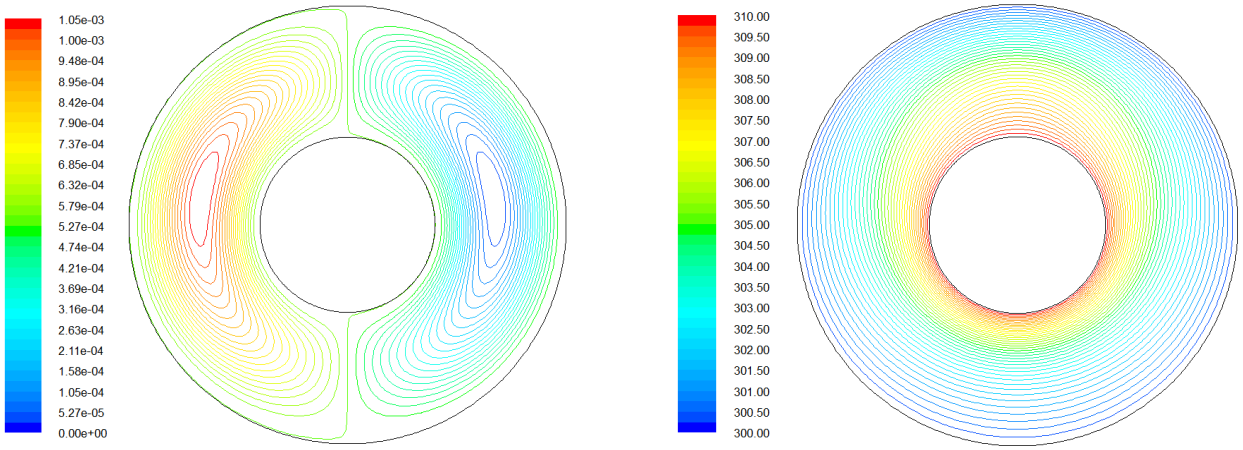

(c)

Streamlines Isotherms

Fig. 4.

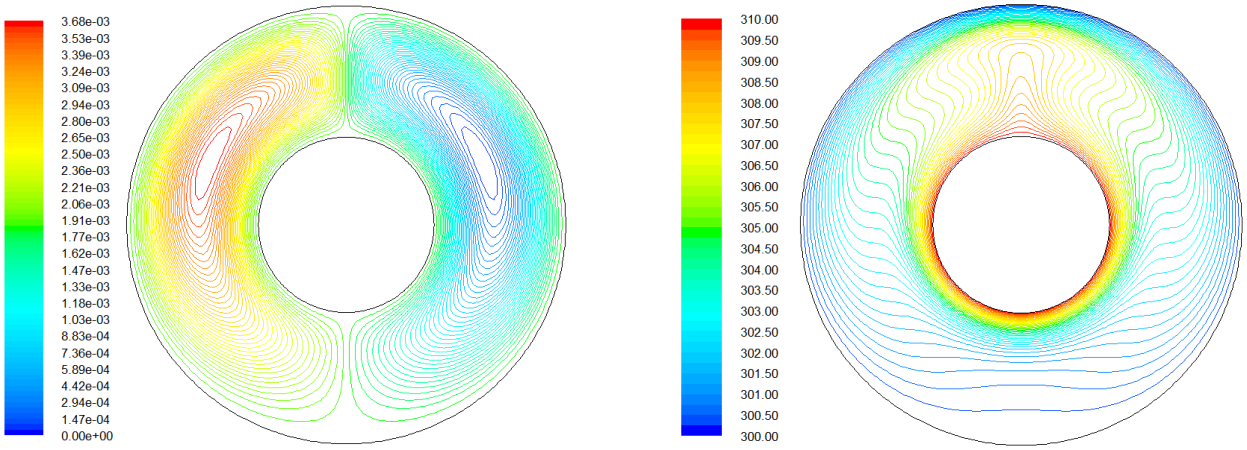

(a)

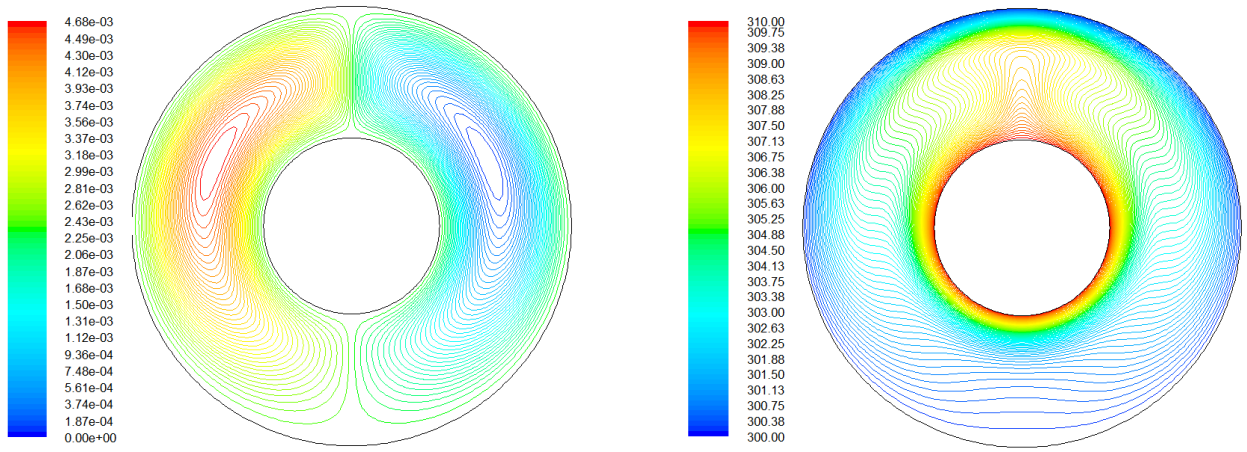

(b)

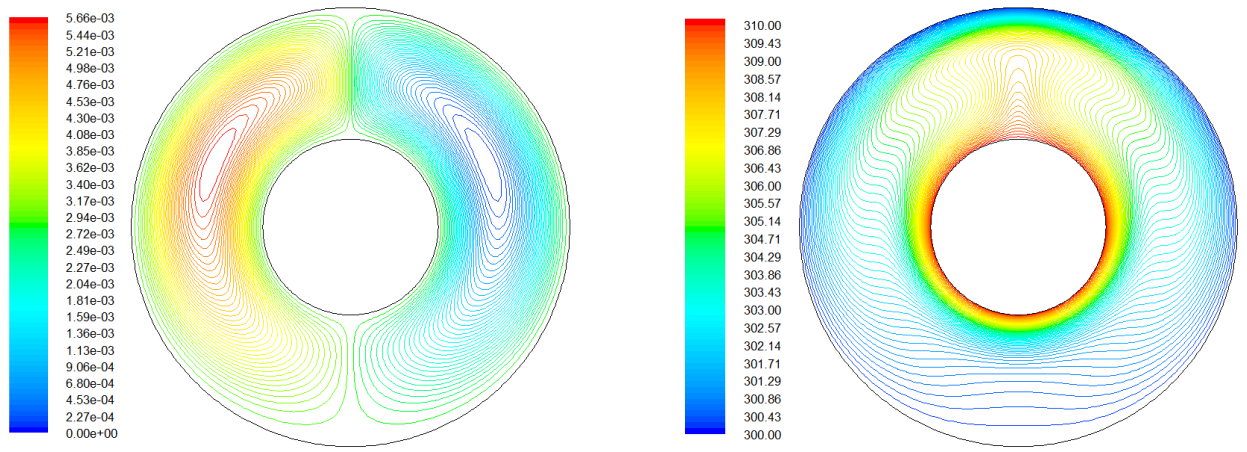

(c)

Streamlines Isotherms

Fig. 5

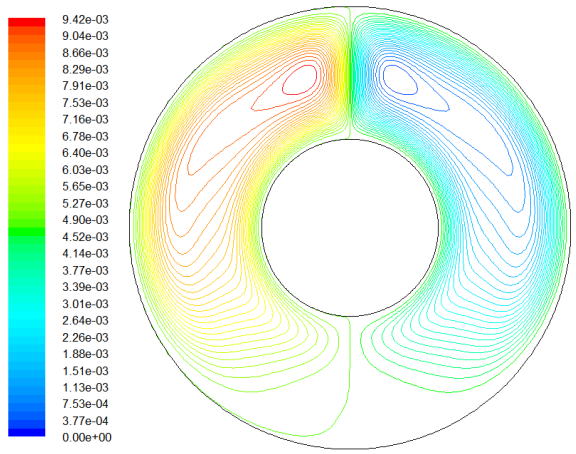

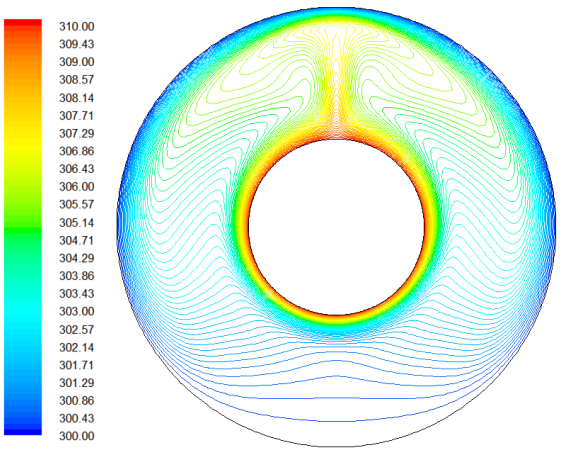

(a)

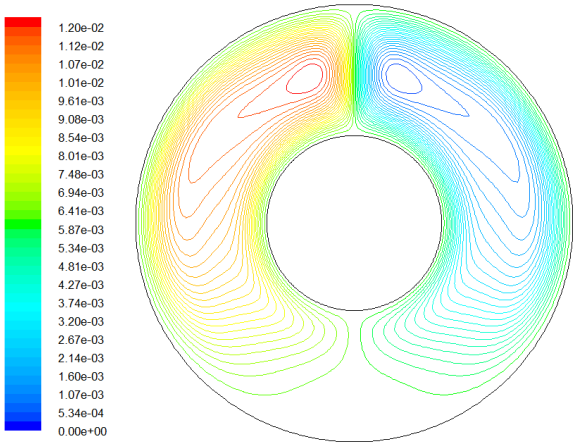

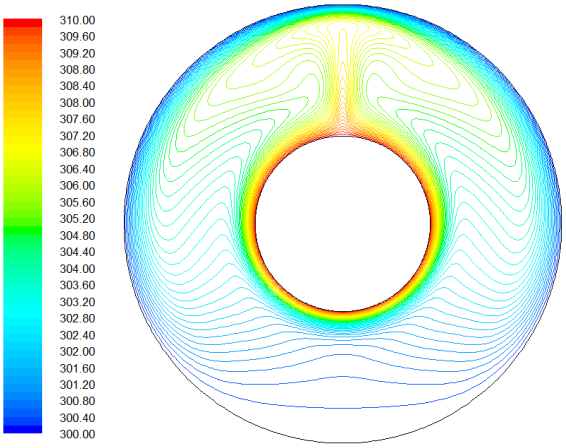

(b)

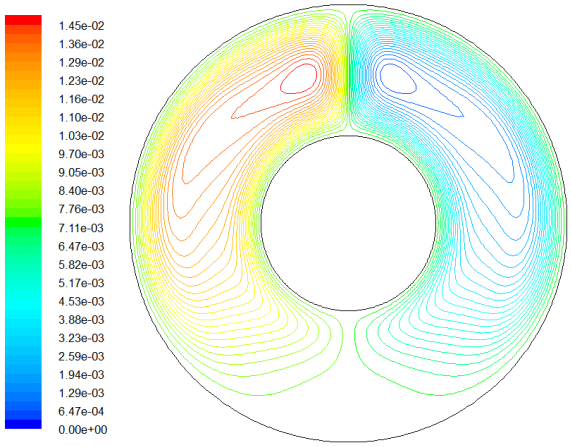

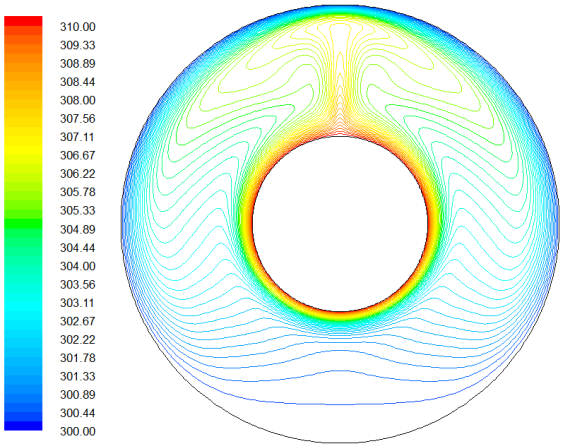

(c)

Streamlines

Isotherms

Fig. 6

Figs. 7(a) and 7(b) show the variation of average Nusselt number versus Fe_3O_4 concentration (φ_M) and CNT concentration (φ_{CNT}), respectively, at different Rayleigh numbers.The average Nusselt number enhances by an increase in any of the parameters of Rayleigh number, Fe_3O_4 concentration and CNT concentration. For example, by increasing the Rayleigh number from 10^3 to 10^5, the average Nusselt number of 0.9%FF and 0.9%FF+1.35%CNT increases by 223.79% and 224.95%, respectively. Additionally, at the Rayleigh number of 10^5, increasing the Fe_3O_4 concentration from 0.5 to 0.9% leads to 7.76% and 18.36% enhancment in the average Nusselt number of 0.9%FF and 0.9%FF+1.35%CNT. According to the obtained results, it can be concluded that merit of using water-Fe_3O_4/CNT hybrid nanofluid to increase the amount of heat transfer in natural convection flow inside a concentric horizontal annulus is higher at greater Rayleigh numbers and nanoparticle concentrations.

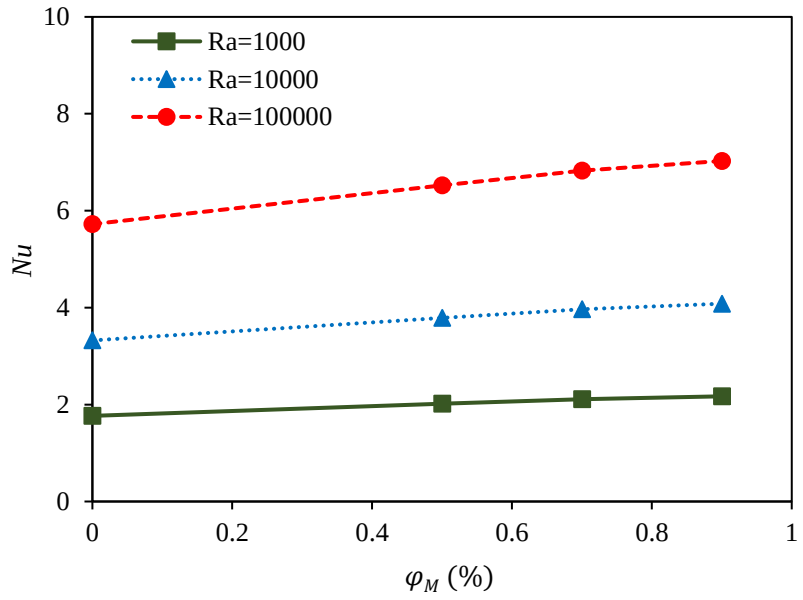

(a)

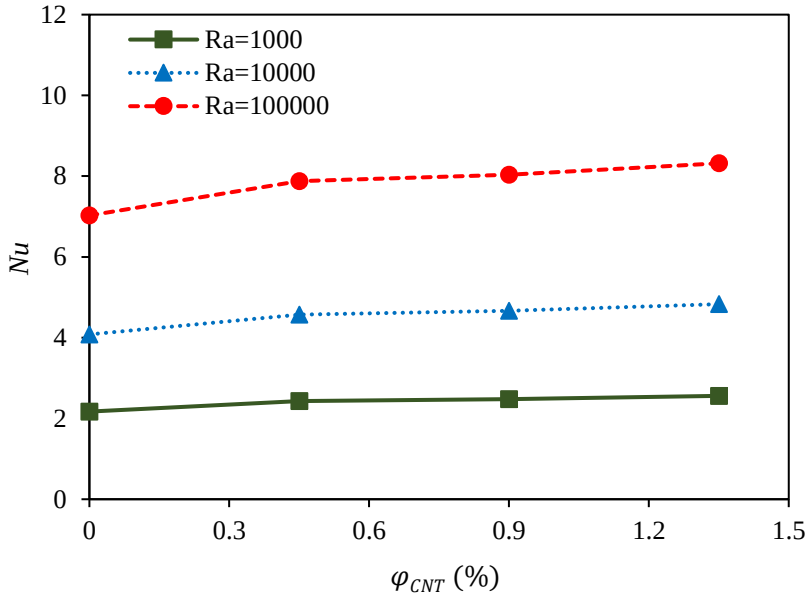

(b)

Fig. 7

Figs. 8(a) and 8(b) illustrate the variation of thermal entropy generation rate versus Fe_3O_4 and CNT concentrations, respectively, at different Rayleigh numbers. It is observed that the thermal entropy generation rate increases with the increase of Rayleigh number at a constant Fe_3O_4 and CNT concentration with a same rate for different nanoparticles. For example, the increase of Rayleigh number from 10^3 to 10^5 leads to 224.98% and 224.65% increase in the thermal entropy generation rate of 0.9%FF and 0.9%FF+1.35%CNT, respectively. According to Eq. (8), the thermal entropy generation rate is a function of thermal conductivity, the average fluid temperature and temperature gradient. As previously mentioned, increasing the Rayleigh number leads to an increase in the heat transfer and, consequently, an increase in the average temperature of the nanofluid, which results in a reduction in the rate of thermal entropy generation. On the other hand, the increase in the Rayleigh number leads to the reduction of the velocity boundary layer thickness and, thus, the reduction of the thermal boundary layer thickness (Bergman et al., 2011). This causes an increase in the temperature gradient and, consequently, an increase in the thermal entropy generation rate. Fig. 8 demonstrates that the

higher temperature gradient effect prevails over the higher average temperature effect and, therefore, the thermal entropy generation rate augments by increasing the Rayleigh number. In addition, Fig. 8 shows that increasing the Fe_3O_4 and CNT concentrations in a constant Rayleigh number leads to an increase in the rate of entropy generation. As an example, at Rayleigh number of 10^5, the increase in Fe_3O_4 concentration from 0 to 0.9% leads to 22.84% and 22.78% enhancement in the entropy generation rate, respectively. The thickness of the velocity boundary layer is constant at a constant Rayleigh number. Besides, the ratio of the velocity and the thermal boundary layer thicknesses are a function of the Prandtl number. Hence, at a constant Rayleigh number, the thermal boundary layer thickness is inversely related to the Prandtl number. The results show that the Prandtl number of the studied nanofluids enhances with the increase of Fe_3O_4 and CNT concentrations. Therefore, at a constant Rayleigh number, the increase of nanoparticle concentration always leads to a decrease in the thermal boundary layer thickness and thus an increase in the thermal entropy generation rate. On the other hand, at a constant Rayleigh number, the increase of nanoparticle concentration leads to an increase in the average temperature and, consequently, a decrease in the thermal entropy generation rate. Fig. 8 reveals that the effect of temperature gradient increment is dominant and, therefore, the thermal entropy generation rate rises by an increase in the nanoparticle concentration.

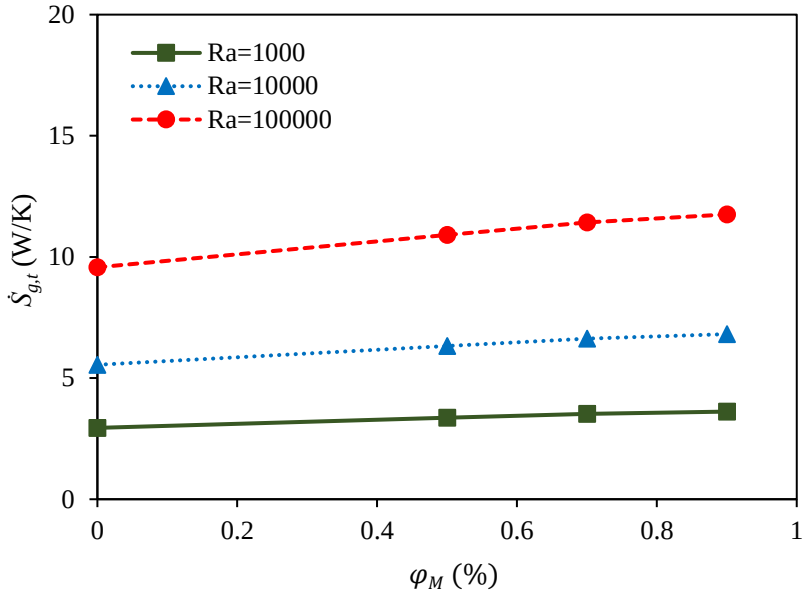

(a)

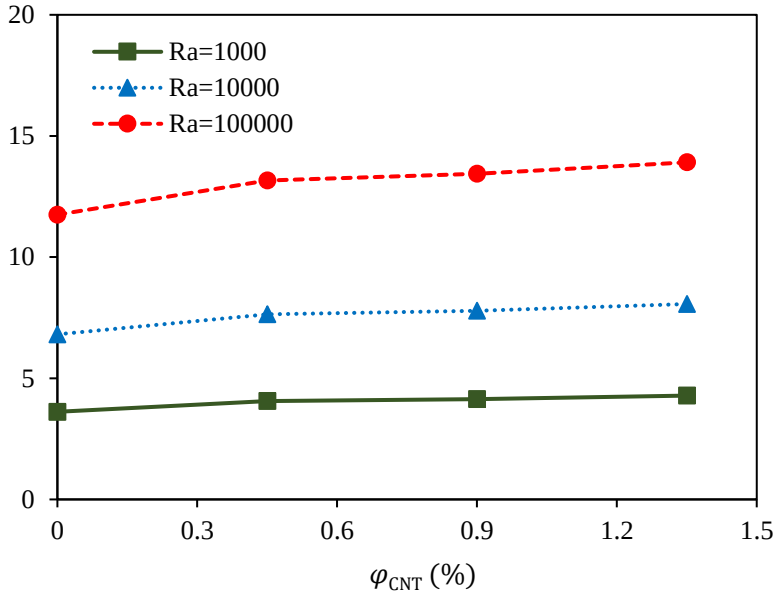

(b)

Fig. 8

Figs. 9(a) and 9(b) display the variation of frictional entropy generation rate versus Fe_3O_4 and CNT concentrations, respectively, at different Rayleigh numbers. It can be seen that the rate of frictional entropy generation increases with increasing the Rayleigh number, Fe_3O_4 concentration and CNT concentration. As an example, increasing the Fe_3O_4 concentration from

0 to 0.9% at Rayleigh numbers of 10^3 and 10^5 leads to 161.95% and 155.25% enhancement in the frictional entropy generation rate, respectively. Moreover, at Rayleigh numbers of 10^3 and 10^5, the frictional entropy generation rate of 0.9%FF+1.35%CNT is 73.79% and 72.7% higher than that for 0.9%FF, respectively. According to Eq. (9), the frictional entropy generation rate is a function of viscosity, the average fluid temperature, and the velocity gradient. At a constant concentration of nanoparticles, increasing the Rayleigh number leads to a decrease in the velocity boundary layer thickness and, consequently, the increase of the velocity gradient, which results in an increase in the frictional entropy generation rate. Furthermore, as mentioned, increasing the Rayleigh number leads to an increase in the average temperature and consequently, a reduction in the frictional entropy generation rate. The results presented in Fig. 9 show that the higher velocity gradient effect prevails over the higher average temperature effect and, therefore, the frictional entropy generation rate augments by increasing the Rayleigh number. In addition, at a constant Rayleigh number, increasing the concentration of nanoparticles leads to an increase in the nanofluid viscosity and the average fluid temperature, which respectively leads to an increase and decrease in the frictional entropy generation rate. However, the effect of increasing the viscosity is higher and therefore the frictional entropy generation rate increases with increasing the concentration of nanoparticles.

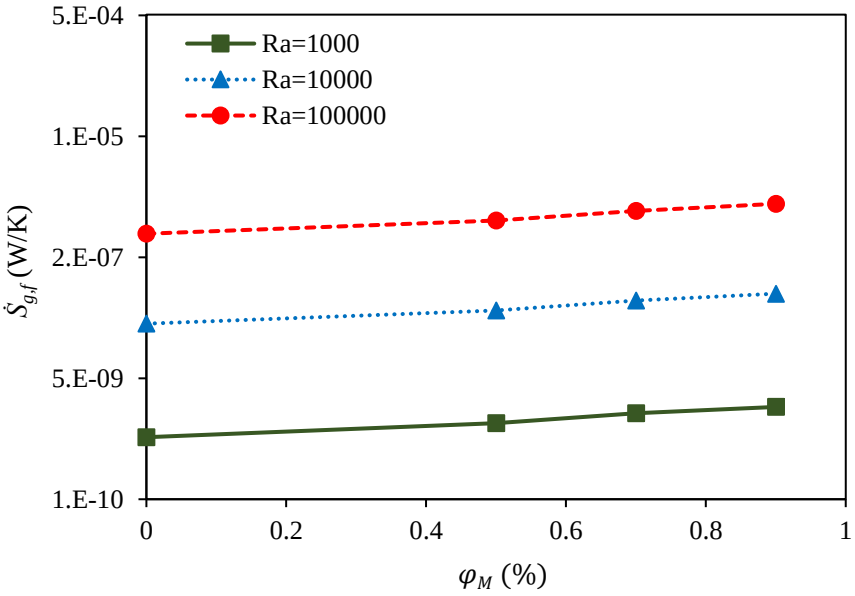

(a)

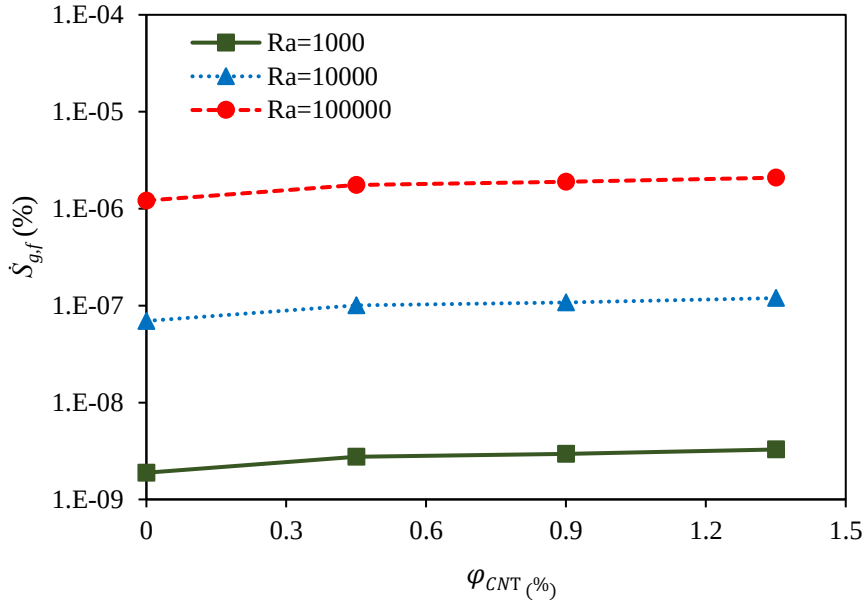

(b)

Fig. 9

The contours of the thermal entropy generation rate (left) and frictional entropy generation rate (right) for the natural convection flow of pure water, 0.9%FF and 0.9%FF+1.35%CNT at the Rayleigh numbers of 10^3, 10^4 and 10^5 are presented in Figs. 10-12, respectively. At the low Rayleigh numbers, most of the thermal entropy is generated in the bottom of the inner cylinder

which is due to the higher temperature gradient in this region. By increasing the Rayleigh number and the formation of the plume region, the natural convection flow is amplified and the fluid rises from the top of the inner cylinder and hits to the outer cylinder. This leads to an increase in the temperature gradient in that area and, consequently, an increase in the thermal entropy generation rate. Furthermore, the contours of the frictional entropy generation rate show that most of the frictional entropy is produced on the left and right sides of the inner cylinder, which is due to the fluid rotation in the kidney-shaped cores. Moreover, an increase in the frictional and thermal entropy generation rates with the concentration of nanoparticles and Rayleigh numbers can be observed in the contours presented in Figs. 10 to 12.

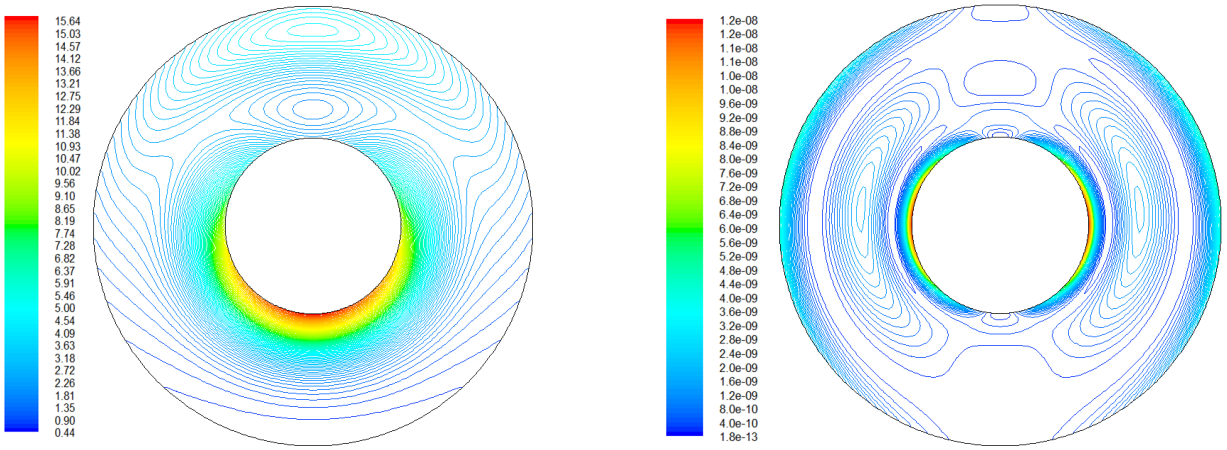

(a)

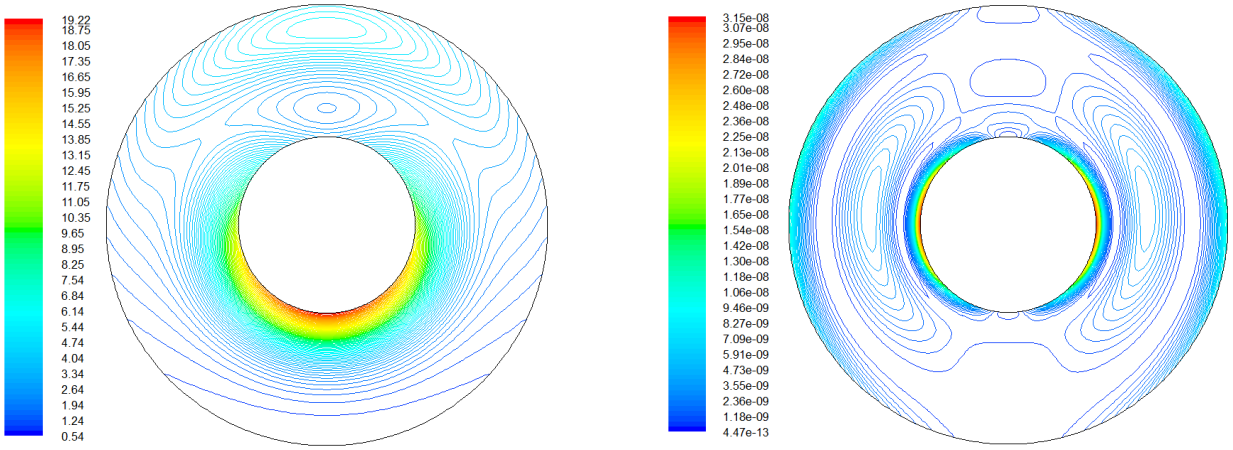

(b)

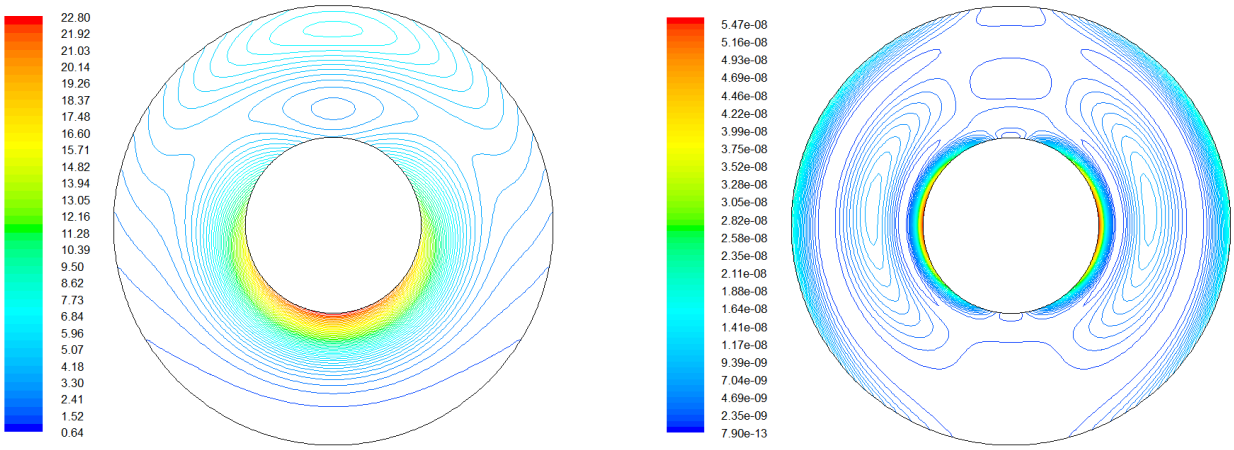

(c)

Thermal entropy generation rate

Frictional entropy generation rate

Fig. 10

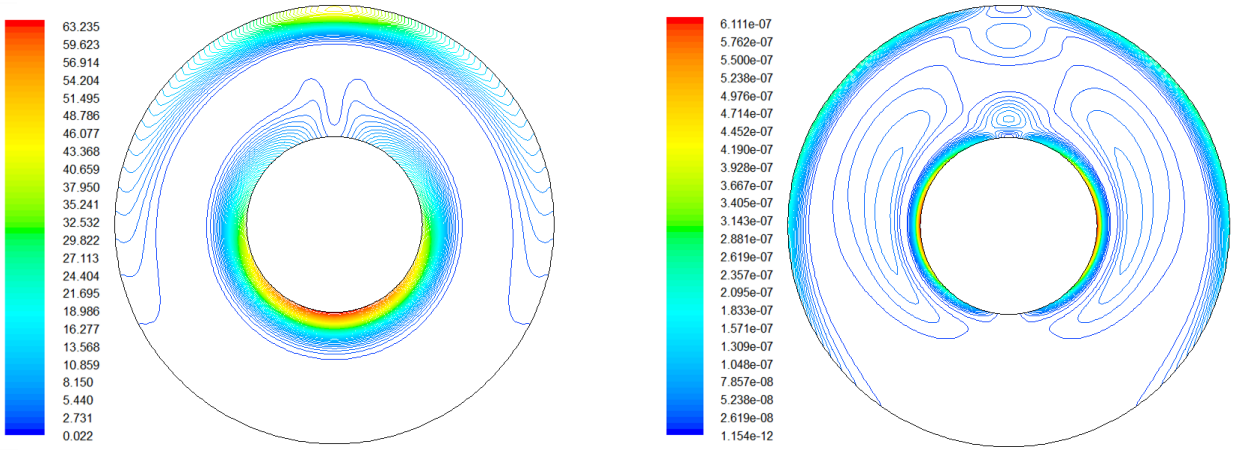

(a)

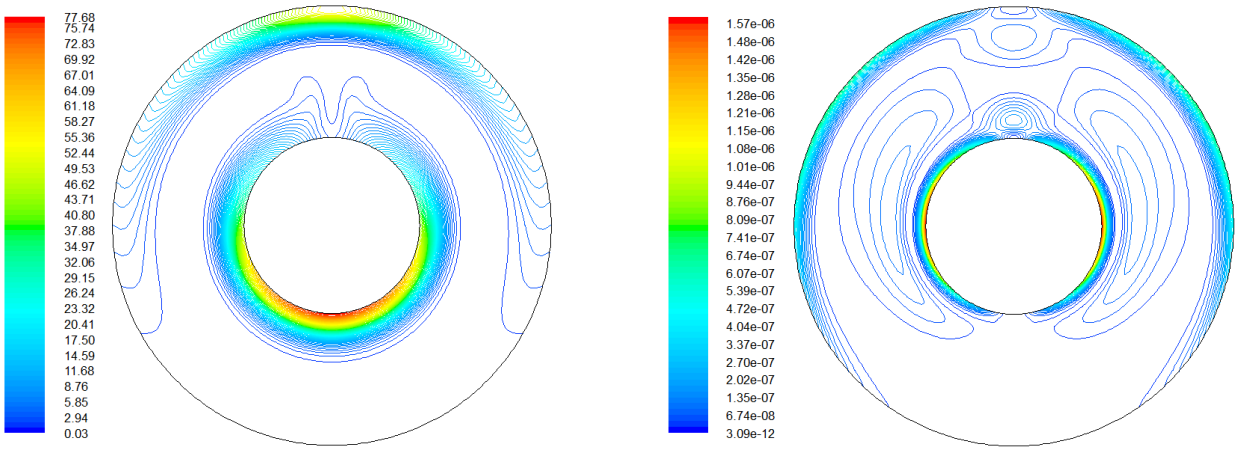

(b)

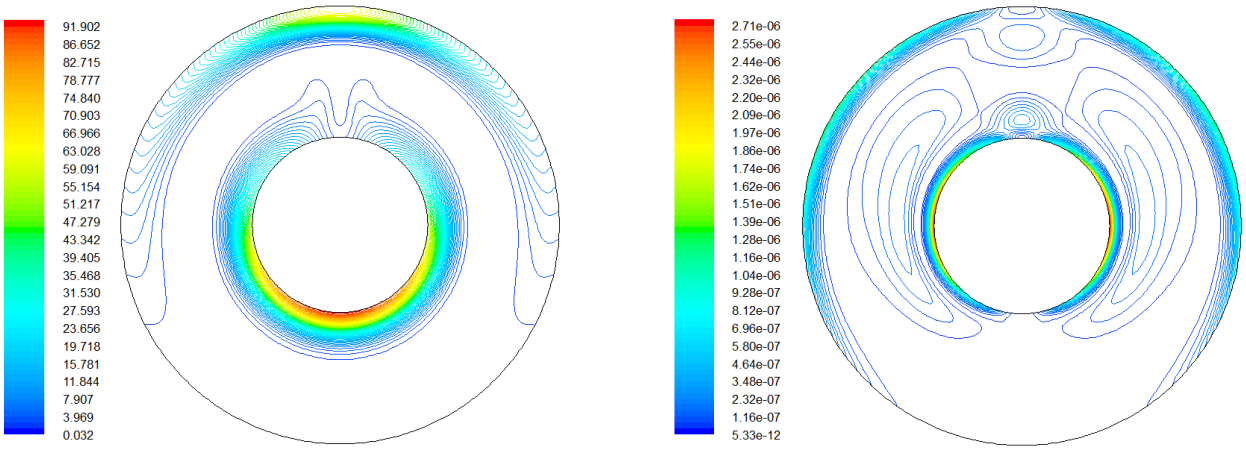

(c)

Thermal entropy generation rate

Frictional entropy generation rate

Fig. 11

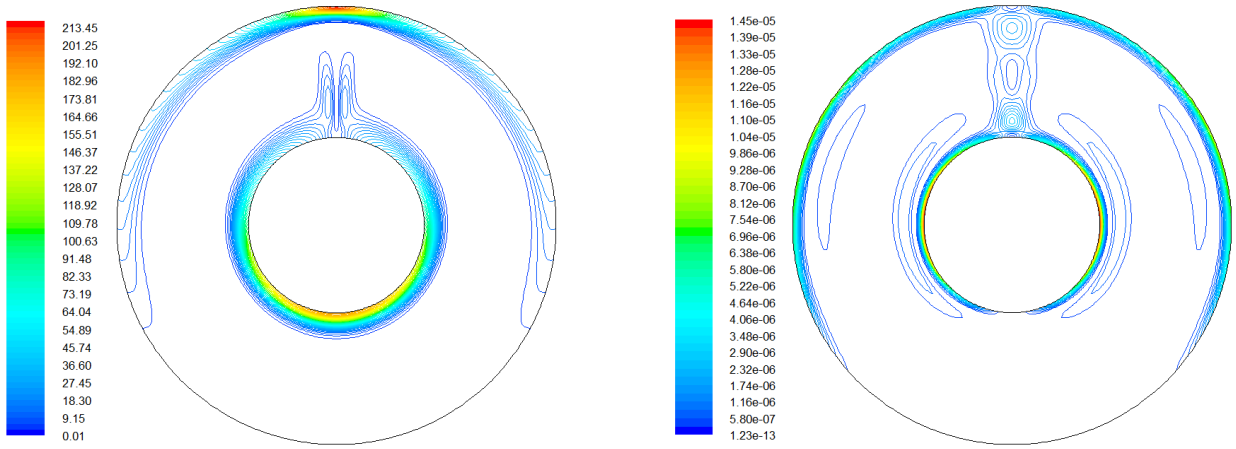

(a)

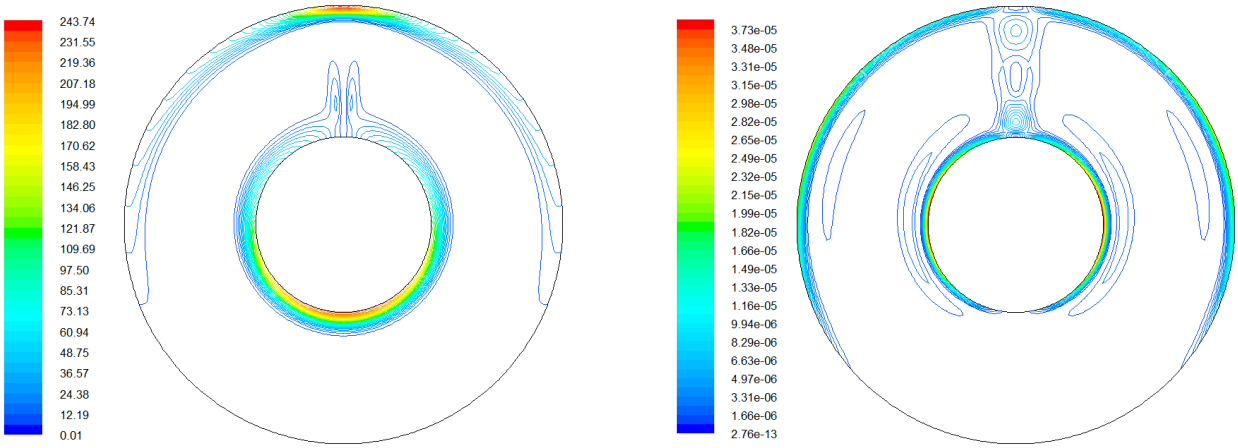

(b)

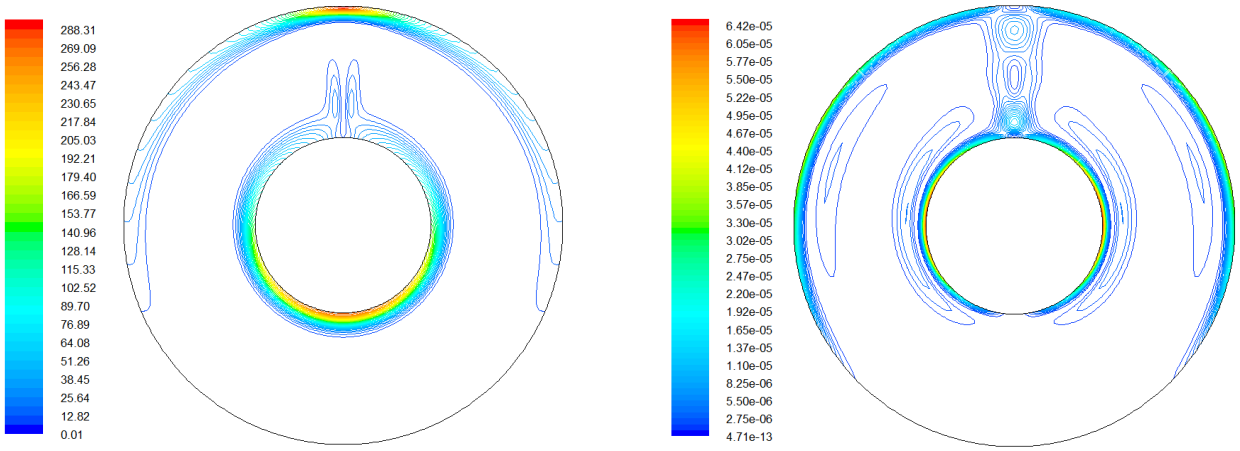

(c)

Thermal entropy generation rate

Frictional entropy generation rate

Fig. 12

Figs. 13(a) and 13(b) show the variation of total entropy generation rate versus Fe_3O_4 and CNT concentrations, respectively, at different Rayleigh numbers. Comparison of the results presented in Figs. 8 and 9 reveals that at the same Rayleigh number and nanoparticle concentrations, the thermal entropy generation rate is much higher than the frictional entropy generation rate. Hence, the trend of changes in the total entropy generation rate is similar to the thermal entropy generation rate. According to the results presented in Fig. 13, it can be concluded that using water-Fe_3O_4/CNT hybrid nanofluid in natural convection flow inside a concentric horizontal annulus is not advantageous from the second-law point of view. Hence, the use of water-Fe_3O_4/CNT nanofluids in natural convection flow in a concentric horizontal annulus depends on whether the designer's goal is to use the nanofluid to increase heat transfer or reduce entropy generation or both.

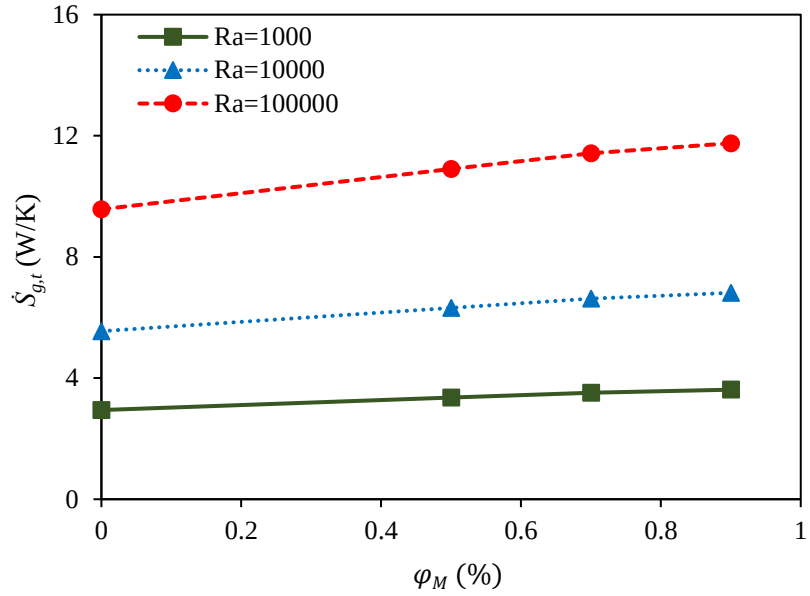

(a)

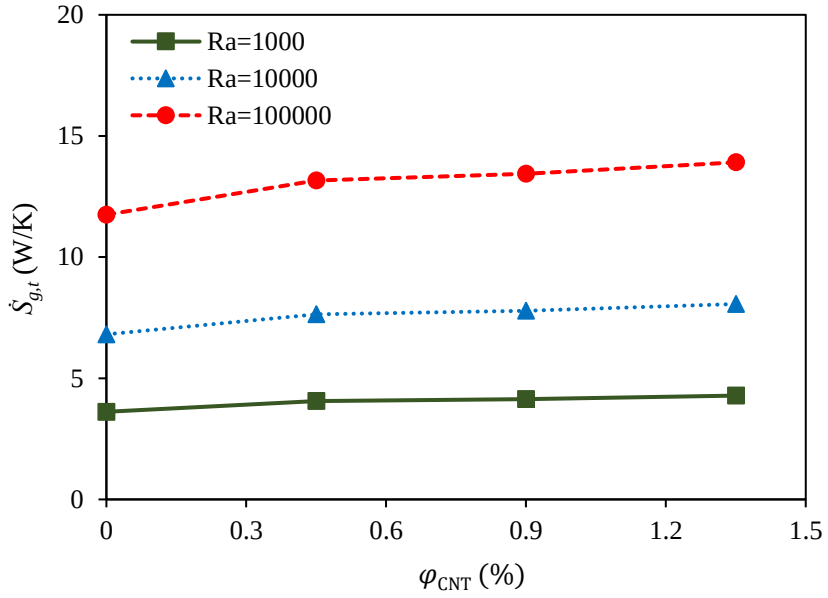

(b)

Fig. 13

5. Conclusion

This numerical research investigates the heat transfer and entropy generation characteristics of the water-Fe_3O_4/CNT hybrid nanofluid in natural convection flow inside a horizontal concentric annulus. The effects of the Fe_3O_4 and CNT volume concentrations and Rayleigh

number on the average Nusselt number as well as the thermal, frictional and total entropy generation rates were investigated. Besides, the effect of these parameters on the streamlines, isotherms and contours of the thermal and frictional entropy generation rates were examined. The results showed that the average Nusselt number increases by increasing the Rayleigh number, Fe_3O_4 concentration and CNT concentration. Furthermore, it was found that the rate of thermal, frictional and total entropy generation augments with an increase in the Fe_3O_4 and CNT concentrations as well as Rayleigh number. However, the rate of thermal entropy generation was much higher than that for the frictional entropy generation. The results of this paper could provide a guideline on the application of newly generated nanofluids in natural convection flows inside the annulus according to both first and second laws of thermodynamics.

References

Abhilash, R. and Lab, S.A. (2018), "Three dimensional analysis of natural convection in a narrow vertical annulus closed at top and opened at bottom", *International Journal of Thermal Sciences*, Vol. 127, pp. 277-287.

Afrand, M. (2017), "Using a magnetic field to reduce natural convection in a vertical cylindrical annulus", *International Journal of Thermal Sciences*, Vol. 118, pp. 12-23.

Berger, P., Adelman, N.B., Beckman, K.J., Campbell, D.J., Ellis, A.B. and Lisensky, G.C. (1999), "Preparation and properties of an aqueous ferrofluid", *Journal of Chemical Education*, Vol. 76, pp. 943.

Bergman, T.L., Lavine, A.S., Incropera, F.P. and DeWitt, D.P. (2011), "Fundamentals of heat and mass transfer", McGraw-Hill, New York.

Cadena-de la Peña, N.L., Rivera-Solorio, C.I., Payán-Rodríguez, L.A., García-Cuéllar, A.J. and López-Salinas, J.L. (2017), "Experimental analysis of natural convection in vertical

annuli filled with AlN and TiO_2/mineral oil-based nanofluids", *International Journal of Thermal Sciences,* Vol. 111, pp. 138-145.

Crawford, L. and Lemlich, R. (1962), "Natural convection in horizontal concentric cylindrical annuli", *Industrial & Engineering Chemistry Fundamentals*, Vol. 1, pp. 260-264.

Dutta, A., Gupta, A.K., Mishra, G., Chhabra, R.P. (2018), "Effect of fluid yield stress and of angle of tilt on natural convection from a square bar in a square annulus", *Computer & Fluids*, Vol. 160, pp. 138-163.

Eckert, E.R.G. and Drake Jr, R.M. (1987), "Analysis of heat and mass transfer", McGraw-Hill, New York.

Garg, P., Alvarado, J.L., Marsh, C., Carlson, T.A., Kessler, D.A. and Annamalai, K. (2009), "An experimental study on the effect of ultrasonication on viscosity and heat transfer performance of multi-wall carbon nanotube-based aqueous nanofluids", *International journal of heat and mass transfer*, Vol. 52, pp. 5090-5101.

Garg, V.K. and Szeri, A.Z. (1992), "Natural convection in a horizontal concentric cylindrical annulus", *International Journal of Numerical Methods for Heat & Fluid Flow*, Vol. 2, pp. 455-467.

Ghernoug, C. , Djezzar, M., Naji, H. and Bouras, A. (2016), "Towards numerical computation of double-diffusive natural convection within an eccentric horizontal cylindrical annulus", *International Journal of Numerical Methods for Heat & Fluid Flow*, vol. 26, pp. 1346-1364.

Imtiaz, H. and Mahfouz, F.M. (2018), "Heat transfer within an eccentric annulus containing heat generating fluid", *International Journal of Heat and Mass Transfer*, Vol. 121, pp. 845-856.

Khanafer, K. and Chamkha, A.J. (2003), "Mixed convection within a porous heat generating horizontal annulus", *International Journal of Heat and Mass Transfer*, Vol. 46, pp. 1725-1735.

Kuhen, T.H. and Goldstein, R.J. (1976), "An experimental and theoretical study of natural convection in the annulus between horizontal concentric cylinders", *Journal of Fluid Mechanics*, Vol. 74, pp. 695-719.

Kuehn, T.H. and Goldstein, R. (1978), "An experimental study of natural convection heat transfer in concentric and eccentric horizontal cylindrical annuli", *Journal of Heat Transfer*, Vol. 100, pp. 635-640.

Li, Z., Sheikholeslami, M., Chamkha, A.J., Raizah, Z.A. and Saleem, S. (2018), "Control volume finite element method for nanofluid MHD natural convective flow inside a sinusoidal annulus under the impact of thermal radiation", *Computer Methods in Applied Mechanics and Engineering*, Vol. 338, pp. 618-633.

Mahmoud Aly, A. and Asai, M. (2016), "ISPH method for double-diffusive natural convection under cross-diffusion effects in an anisotropic porous cavity/annulus", *International Journal of Numerical Methods for Heat & Fluid Flow*, Vol. 26, pp. 235-268.

Parvin, S., Nasrin, R., Alim, M., Hossain, N. and Chamkha, A.J. (2012), "Thermal conductivity variation on natural convection flow of water–alumina nanofluid in an annulus", *International journal of heat and mass transfer*, Vol. 55, pp. 5268-5274.

Putra, N., Roetzel, W. and Das, S.K. (2003), "Natural convection of nanofluids", *Heat and Mass Transfer*, Vol. 39, pp. 775-784.

Selimefendigil, F. and Oztop, H.F. (2017), "Conjugate natural convection in a nanofluid filled partitioned horizontal annulus formed by two isothermal cylinder surfaces under magnetic field", *International Journal of Heat and Mass Transfer*, Vol. 108, pp. 156-171.

Shahsavar, A., Saghafian, M., Salimpour, M.R. and Shafii, M. (2016), "Experimental investigation on laminar forced convective heat transfer of ferrofluid loaded with carbon nanotubes under constant and alternating magnetic fields", *Experimental Thermal and Fluid Science*, Vol. 76, pp. 1-11.

M. Siavashi, A. Rostami, "Two-phase simulation of non-Newtonian nanofluid natural convection in a circular annulus partially or completely filled with porous media", International Journal of Mechanical Sciences, 133 (2017) 689-703.

Vadasz, J.J., Govender, S. and Vadasz, P. (2005), "Heat transfer enhancement in nanofluids suspensions: possible mechanisms and explanations", *International journal of heat and mass transfer*, Vol. 48, pp. 2673-2683.

Zhao, M., Yu, D.M., Zhang, Y., "Evolution to chaotic natural convection in a horizontal annulus with an internally slotted circle", *International Journal of Heat and Mass Transfer*, Vol. 126, pp. 95-108.

Afrand, M., D. Toghraie, A. Karimipour and S. Wongwises (2017). "A numerical study of natural convection in a vertical annulus filled with gallium in the presence of magnetic field." Journal of Magnetism and Magnetic Materials **430**: 22-28.

Akbari, O. A., D. Toghraie and A. Karimipour (2015). "Impact of ribs on flow parameters and laminar heat transfer of water–aluminum oxide nanofluid with different nanoparticle volume fractions in a three-dimensional rectangular microchannel." Advances in Mechanical Engineering **7**(11): 1687814015618155.

Akbari, O. A., D. Toghraie, A. Karimipour, A. Marzban and G. R. Ahmadi (2017). "The effect of velocity and dimension of solid nanoparticles on heat transfer in non-Newtonian nanofluid." Physica E: Low-dimensional Systems and Nanostructures **86**: 68-75.

Akbari, O. A., D. Toghraie, A. Karimipour, M. R. Safaei, M. Goodarzi, H. Alipour and M. Dahari (2016). "Investigation of rib's height effect on heat transfer and flow parameters of laminar water–Al2O3 nanofluid in a rib-microchannel." Applied Mathematics and Computation **290**: 135-153.

Alipour, H., A. Karimipour, M. R. Safaei, D. T. Semiromi and O. A. Akbari (2017). "Influence of T-semi attached rib on turbulent flow and heat transfer parameters of a silver-water nanofluid with different volume fractions in a three-dimensional trapezoidal microchannel." Physica E: Low-dimensional Systems and Nanostructures **88**: 60-76.

Arabpour, A., A. Karimipour and D. Toghraie (2018). "The study of heat transfer and laminar flow of kerosene/multi-walled carbon nanotubes (MWCNTs) nanofluid in the microchannel heat sink with slip boundary condition." Journal of Thermal Analysis and Calorimetry **131**(2): 1553-1566.

Arabpour, A., A. Karimipour, D. Toghraie and O. A. Akbari (2018). "Investigation into the effects of slip boundary condition on nanofluid flow in a double-layer microchannel." Journal of Thermal Analysis and Calorimetry **131**(3): 2975-2991.

Heydari, M., D. Toghraie and O. A. Akbari (2017). "The effect of semi-attached and offset mid-truncated ribs and Water/TiO2 nanofluid on flow and heat transfer properties in a triangular microchannel." Thermal Science and Engineering Progress **2**: 140-150.

Mashayekhi, R., E. Khodabandeh, M. Bahiraei, L. Bahrami, D. Toghraie and O. A. Akbari (2017). "Application of a novel conical strip insert to improve the efficacy of water–Ag nanofluid for utilization in thermal systems: A two-phase simulation." Energy Conversion and Management **151**: 573-586.

Pourfattah, F., M. Motamedian, G. Sheikhzadeh, D. Toghraie and O. Ali Akbari (2017). "The numerical investigation of angle of attack of inclined rectangular rib on the turbulent heat

transfer of Water-Al2O3 nanofluid in a tube." International Journal of Mechanical Sciences **131-132**: 1106-1116.

Rezaei, O., O. A. Akbari, A. Marzban, D. Toghraie, F. Pourfattah and R. Mashayekhi (2017). "The numerical investigation of heat transfer and pressure drop of turbulent flow in a triangular microchannel." Physica E: Low-dimensional Systems and Nanostructures **93**: 179-189.

Sajadifar, S. A., A. Karimipour and D. Toghraie (2017). "Fluid flow and heat transfer of non-Newtonian nanofluid in a microtube considering slip velocity and temperature jump boundary conditions." European Journal of Mechanics - B/Fluids **61**: 25-32.

Shamsi, M. R., O. A. Akbari, A. Marzban, D. Toghraie and R. Mashayekhi (2017). "Increasing heat transfer of non-Newtonian nanofluid in rectangular microchannel with triangular ribs." Physica E: Low-dimensional Systems and Nanostructures **93**: 167-178.

Zadkhast, M., D. Toghraie and A. Karimipour (2017). "Developing a new correlation to estimate the thermal conductivity of MWCNT-CuO/water hybrid nanofluid via an experimental investigation." Journal of Thermal Analysis and Calorimetry 129(2): 859-867.

Igor V. Miroshnichenko, Mikhail A. Sheremet, Hakan F. Oztop, Nidal Abu-Hamdeh, Natural convection of Al2O3/H2O nanofluid in an open inclined cavity with a heat-generating element, International Journal of Heat and Mass Transfer, 126 (2018) 184–191.

Figure captions

Fig. 1. Schematic of the studied problem.

Fig. 2. Structured non-uniform grid for the computational domain.

Fig. 3. Comparison of present temperature profiles (solid lines) with experimental results reported by Kuhen and Goldstein (1976) (symbols) for flow of water in an concentric annulus using $Ra = 4.57 \times 10^4$, $Pr = 0.7$ and $\frac{r_o - r_i}{2r_i} = 0.8$.

Fig. 4. The streamlines (left) and isotherms (right) for the natural convection flow of (a) pure water, (b) 0.9% FF and (c) 0.9% FF+1.35%CNT at $Ra = 10^3$.

Fig. 5. The streamlines (left) and isotherms (right) for the natural convection flow of (a) pure water, (b) 0.9% FF and (c) 0.9% FF+1.35%CNT at $Ra = 10^4$.

Fig. 6. The streamlines (left) and isotherms (right) for the natural convection flow of (a) pure water, (b) 0.9% FF and (c) 0.9% FF+1.35%CNT at $Ra = 10^5$.

Fig. 7. Average Nusselt number at different Rayleigh numbers in terms of (a) Fe_3O_4 concentration and (b) CNT concentration.

Fig. 8. Thermal entropy generation rate at different Rayleigh numbers in terms of (a) Fe_3O_4 concentration and (b) CNT concentration.

Fig. 9. Frictional entropy generation rate at different Rayleigh numbers in terms of (a) Fe_3O_4 concentration and (b) CNT concentration.

Fig. 10. The contours of the thermal (left side) and frictional (right) entropy generation rates for the natural convection flow of (a) pure water, (b) 0.9% FF and (c) 0.9% FF+1.35%CNT at $Ra = 10^3$.

Fig. 11. The contours of the thermal (left side) and frictional (right) entropy generation rates for the natural convection flow of (a) pure water, (b) 0.9% FF and (c) 0.9% FF+1.35%CNT at $Ra = 10^4$.

Fig. 12. The contours of the thermal (left side) and frictional (right) entropy generation rates for the natural convection flow of (a) pure water, (b) 0.9% FF and (c) 0.9% FF+1.35%CNT at $Ra = 10^5$.

Fig. 13. Total entropy generation rate at different Rayleigh numbers in terms of (a) Fe_3O_4 concentration and (b) CNT concentration.